Journal of Applied Fluid Mechanics, Vol. 11, No. 3, pp. 637-645, 2018.
Available online at www.jafmonline.net, ISSN 1735-3572, EISSN 1735-3645.
DOI: 10.29252/jafm.11.03.28531

A Similarity Solution with Two-Equation Turbulence Model for Computation of Turbulent Film Condensation on a Vertical Surface

M. Ziaei-Rad[1†], A. Ahmadi Nadooshan[2] and S. Mahmoodi[2]

[1] *Department of Mechanical Engineering, Faculty of Engineering, University of Isfahan, Isfahan, Iran*
[2] *Department of Mechanical Engineering, Faculty of Engineering, Shahrekord University, Shahrekord, Iran*

†*Corresponding Author Email:m.ziaeirad@eng.ui.ac.ir*

(Received October 20, 2017; accepted December 12, 2017)

ABSTRACT

In this paper, we presented a similarity solution for turbulent film condensation of stationary vapor on an isothermal vertical flat plate. In this method, some similarity transformations are employed and the set of governing partial differential equations (PDE) of conservation together with transport equations of turbulent kinetic energy and dissipation rate are transformed into a set of ordinary differential equations (ODE). Calculated data for the flow field, velocity profile, wall shear stress, condensate film thickness, turbulent kinetic energy, rate of dissipation, and heat transfer properties are discussed. The effect of Prandtl (Pr) number was also investigated in a wide range of variations. The obtained results showed that at high Prandtl numbers, the velocity profile becomes more uniform across the condensation film and therefore, the kinetic energy of turbulence is reduced. Furthermore, the effect of change in Pr is negligible at high Pr numbers and consequently, the flow parameters have no significant change in this range. The friction coefficient changes linearly through the condensation film and the slope of friction lines diminishes slightly by the Pr number. The rate of turbulent kinetic energy increases linearly from the wall up to about 20% of condensate film, then rises asymptotically and converges to a constant value near the liquid-vapor interface. Also, the rate of turbulent dissipation grows linearly up to 40% of condensate film thickness and then increases slightly while it oscillates.

Keywords: Turbulent film condensation; Similarity solution; k-ε turbulence modeling; Vertical surface.

NOMENCLATURE

a,b,c,d,e	coefficients
C	constant
C_p	heat capacity
E	dimensionless turbulent dissipation rate
F	stream function
g	gravitational acceleration
h_{fg}	latent heat transfer coefficient
Ja	Jacob number
K	dimensionless turbulent kinetic energy
k	turbulent kinetic energy
m,n,p,q,l	constant powers
Pr	Prandtl number
T	temperature
u,v	velocity components
x,y	stream/normal directions
δ	boundary layer edge
ε	turbulent dissipation rate
η	similarity variable
θ	dimensionless temperature
λ	conductivity
ν_t	eddy viscosity
ρ	density
σ	constant
ψ	stream function

1. INTRODUCTION

Because of phase change and the basic role of latent heat, heat transfer occurs in constant temperature in film condensation. In fact in condensation, the heat is transferred with high rate and low temperature difference. Therefore, condensation plays a significant role in numerous engineering designs such as power plants, chemical engineering, medical industry and air conditioning. However, in most of these applications, the condensate film becomes turbulent after a short distance.

Several analytical and numerical methods can be found in literatures for formulation and solution of

two-phase flows (in particular, the problem of film condensation) governing equations. A common scheme is the 'integral method' in which the governing equation for liquid and vapor phases are derived separately and then the results are obtained by integrating the equations over a specific range. In this method, the formulation is relatively simple, but applying the boundary conditions and solving the resultant integrals is difficult. Another method is to solve directly the flow field governing PDEs using a numerical scheme. However, due to the presence of two different phases, the solution procedure and applying the boundary conditions are very complicated in this method and it consumes considerable CPU and time. There is also a well-known notable method for complex problems called similarity solution. In this approach, it is possible to change the set of governing PDEs into ordinary differential equations (ODE) by applying an appropriate similarity variable. Thus, the number of independent variables is reduced which results in an easy solution for the equations and relatively simple applying of boundary conditions. However, the method is limited to free or force convection flows on physically simple geometries (Kays *et al.* 2012).

The first study on laminar film condensation of stagnant vapor is published by Nusselt (Incropera and DeWitt 2007). After Nusselt work, numerous studies have been made on the laminar film condensation of a quiescent vapor on various geometries. Sparrow and Gregg (1959) used a similarity solution to analyze the full boundary layer equations for condensate film. They showed that the condensate film thickness is dependent on physical quantity $C_p\Delta T/h_{fg}$, known as Jacob number. In low Jacob numbers, their results correlated with Nusselt theory. Koh *et al.* (1961) solved two set of governing equations for liquid and vapor phase, simultaneously. They adopted the shear effects on liquid-vapor interface and indicated that it is satisfactory to neglect them in governing equations. Chen *et al.* (1961) investigated laminar film condensation of pure vapor on vertical flat plate experimentally. They also noted that the shear layer is negligible at liquid-vapor interface. The Nusselt theory correlates their experimental data at Reynolds numbers lower than 20. Mendez *et al.* (2000) numerically analyzed laminar film condensation on a two-dimensional fin. They solved conduction heat transfer in fin and phase changing of vapor and showed that in fins with high thermal conductivity, the results coincide with Nusselt theory and when conductivity becomes smaller than a critical point, it is possible that some area on the fin becomes dried and hence, condensation may not occur. Shekrilazde and Gomelauri (1966) studied film condensation on low velocity flowing vapor on horizontal tubes. They used an asymptotic solution to model shear effect on vapor-liquid interface. Their results could correlate experimental data at low velocities but n increased velocity, deviance grows, and the model did not respond favorably for high velocities. Sosnowski *et al.* (2013) investigated laminar film condensation of stagnant vapor-air mixture on solid surfaces with different substances. They used OpenFOAM to solve governing equations and showed that vapor concentration in mixture in the presence of metals is much less than non-metallic substances, therefore, the condensation rate increases on surfaces with high thermal conductivity. There are also some previous studies on using nanofluids in the condensate layer (Avramenko *et al.* 2014, 2015; Liu *et al.* 2010; Gabriela and Angel Huminic 2013).

Available published literatures provide a wide investigation on laminar film condensation. But in the case of turbulent film condensation, cause of complications in two-phase turbulent flows, experimental works are much more than numerical studies. However, numerical analysis of turbulent film condensation is also of interest (Lee 1964; Kharangate and Mudawar 2017). Koyama (1984) analyzed turbulent film condensation on a horizontal tube. They neglected the shear effects in vapor-liquid interface and solved the governing equations numerically using integration method. Their results revealed that heat transfer rate increases with distance from the upper stagnant point and decreases toward downer stagnant point. They also showed that heat transfer rate due to condensation on vertical plates are always more than those of tubes. Michael *et al.* (1989) presented an important concept on film condensation in which they suggested that the flow in condensate film is partially turbulent. This is caused by wave forming in film condensation phenomena. Nakayama and Koyama (1984) and Sarma *et al.* (1998) formulated turbulent film condensation of flowing air-vapor mixture with high velocity on a horizontal tube. They neglected inertia terms in momentum and energy equations. They used Kato's eddy diffusivity model to model the eddy viscosity (Kato *et al*. 1968) and used Colburn analogy to calculate the interfacial shear effect. They showed that the maximum local Nusselt number is at the angle of 90º on the tube (where the effect of gravity is maximum), and that the condensate film thickness increases at high velocities. Sheng and Yan-Ting (2005) added the pressure gradient from potential flow, omitted the inertial terms and adopted the separation for turbulent film condensation of moving vapor on a horizontal tube. They demonstrated that when the velocity of vapor increases, the film thickness grows and the separation point moves toward the upper region. Cha'o-Kuang and Yan-Ting (2009) analyzed turbulent film condensation of vapor in the presence of non-condensable gas on a circular tube. They solved the governing equation in two-phase using finite different implicit method. They used Kato's model to calculate the eddy diffusivity, and showed that in the presence of small amount of non-condensable gas, the Nusselt number takes a large negative change.

Recently, Cintolesi *et al.* (2017) utilized large-eddy simulation to study a hot and wet plate surrounded by a cold and wet square enclosure. They reported

the evolution of the drying-process simulations and concluded that the physical properties of the plate materials lead to different decays of the surface thermal fluctuations. Gou *et al.* (2017) developed an analytical model for pure vapor condensation in a vertical tube. They recommended Kay's turbulent eddy diffusivity model for their newly proposed model and claimed that there is a good agreement between their results and available experimental data. Shen *et al.* (2017) proposed an improved model amplifying the thermal conductivity of vapor in the phase interaction region and showed that the interfacial temperature deviation is reduced by the amplified thermal conductivity of vapor. Swartz and Yao (2017) experimentally investigated the influence of film waviness and mass transfer suction on the turbulent, natural convective condensing flow with high non-condensable mass fraction. Their test results showed a significant enhancement in heat transfer caused by disruption of the gas boundary layer due to film waviness. They also proposed a new correlation and compared the results to several datasets.

There are a few studies in literatures on similarity solution of turbulent flow, which are for some cases excluding the problem of condensation. Principally, finding appropriate similarity variables to change the governing equations of turbulent flow into ODEs is a complex process. In contrast, if we succeed to do so by applying valid assumptions, the solution procedure will be easier and the computational cost is reduced considerably. Paullay *et al.* (1985) utilized similarity method to solve turbulent flow of planar and circular jets. They stated that due to special boundary conditions, singular points exist in PDEs as well as obtained ODEs of the problem. As a result, regular numerical schemes are not applicable in this case and a secondary transformation is required to transfer the singular points to infinity and solve the equations asymptotically. Wen-xin and Li (1993) investigated the problem of turbulent natural convection near a solid wall. They employed two-equation k-ε model for turbulence modeling, and then introduced a proper similarity variable to achieve ODEs and finally, solved them by space marching.

The above reviewed studies used similarity solution for single-phase flows with constant properties. Furthermore, they replaced simplified asymptotic method with limited range of validity in the numerical schemes. Therefore, the lack of a comprehensive similarity solution for the problem of turbulent film condensation is obvious in literatures. Usually, it is difficult to investigate two-phase flow problems via solving the governing PDEs, whereas solution and making discussion on the set of transformed ODEs are more amenable. In this paper, by introducing some useful transformation variables, we change the formidable set of governing conservation PDEs together with two transport equations for turbulence quantities into a set of ODEs. We also use a wide range of Prandtl number and govern the problem of presence of singular points in the equations through a suitable numerical technique.

2. PHYSICAL MODEL AND ASSUMPTIONS

Figure 1 shows a schematic of turbulent film condensate flowing on a vertical flat plate. Infinite stationary bulk vapor has its saturated temperature, therefore there is no temperature gradient and interface surface attains saturated temperature. Flat plate is at uniform constant temperature T_w. It is assumed that plate is much bigger than condensate thickness, therefore it is allowable to formulate equations in two dimensional coordinate, and turbulent flow appears at the top of the plate.

According to no slip condition on the wall, there is no tangential or vertical component of velocity there. Moreover, turbulent kinetic energy, k, and its dissipation rate, ε, are set to be zero on the surface, since the vapor is in quiescent state with no disturbance. Also, the gradient of k and ε take zero at the liquid-vapor interface surface.

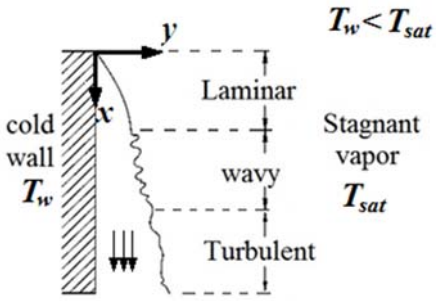

Fig. 1. Physical model of turbulent film condensation on a vertical surface.

Considering boundary layer approximations, the axial diffusion terms can be neglected in the governing equations. Also, y-momentum equation is reduced to $\partial p/\partial y = 0$, confirming that the pressure in the condensate layer is a function of flow direction (x) only and can be expressed in terms of density change. Therefore, we can write the equations of continuity, x-momentum, energy, turbulent kinetic energy and its dissipation rate, as follow:

$$\frac{\partial u}{\partial x} + \frac{\partial v}{\partial y} = 0 \tag{1}$$

$$u\frac{\partial u}{\partial x} + v\frac{\partial u}{\partial y} = \frac{(\rho_l - \rho_v)}{\rho_l}.g + \frac{\partial}{\partial y}\left(\nu_t \frac{\partial u}{\partial y}\right) \tag{2}$$

$$u\frac{\partial T}{\partial x} + v\frac{\partial T}{\partial y} = \frac{\partial}{\partial y}\left(\frac{\nu_t}{\sigma_t}\frac{\partial T}{\partial y}\right) \tag{3}$$

$$u\frac{\partial k}{\partial x} + v\frac{\partial k}{\partial y} = \frac{\partial}{\partial y}\left(\frac{\nu_t}{\sigma_k}\frac{\partial k}{\partial y}\right) + \nu_t\left(\frac{\partial u}{\partial y}\right)^2 - \varepsilon \tag{4}$$

$$u\frac{\partial \varepsilon}{\partial x} + v\frac{\partial \varepsilon}{\partial y} = \frac{\partial}{\partial y}\left(\frac{\nu_t}{\sigma_\varepsilon}\frac{\partial \varepsilon}{\partial y}\right) + c_1\frac{\varepsilon}{k}\nu_t\left(\frac{\partial u}{\partial y}\right)^2 - c_2\frac{\varepsilon^2}{k} \tag{5}$$

Here u and v are the velocity components in streamwise (x) and normal (y) directions, respectively. T is temperature, g is gravity, and ρ_l and ρ_v respectively define the liquid and vapor

densities. Moreover, turbulent kinetic energy and its dissipation rate are denoted by k and ε, respectively, and ν_t is the eddy viscosity, expressed as:

$$\nu_t = C_\mu \frac{k^2}{\varepsilon} \tag{6}$$

The model constants take the below (Wilcox, 1994):

$$\sigma_t = 0.9, \quad \sigma_k = 1.0, \quad \sigma_\varepsilon = 1.3$$
$$C_1 = 1.44, \quad C_2 = 1.92, \quad C_\mu = 0.09 \tag{7}$$

Finally, the boundary conditions are defined as:

$$y = 0: \begin{cases} u = 0 \\ v = 0 \\ T = T_w \\ k = 0 \\ \varepsilon = 0 \end{cases}, \quad y \to \delta: \begin{cases} \frac{\partial u}{\partial y} = 0 \\ T = T_{sat} \\ \frac{\partial k}{\partial y} = 0 \\ \frac{\partial \varepsilon}{\partial y} = 0 \end{cases} \tag{8}$$

2.1 Similarity Analysis

To derive the ordinary differential equations from governing partial differential Eqs. (1-5), we define appropriate similarity variables as below:

$$\eta = a\, x^{-l}\, y \tag{9}$$

$$\psi = b\, x^m\, F(\eta) \tag{10}$$

$$c\, x^n \theta(\eta) = \frac{T_{sat} - T}{T_{sat} - T_w} \tag{11}$$

$$k = d\, x^p\, K(\eta) \tag{12}$$

$$\varepsilon = e\, x^q\, E(\eta) \tag{13}$$

where, ψ is the stream function, defined by $u = \partial\psi/\partial y, v = -\partial\psi/\partial x$, and η, F, θ, K and E are non-dimensional forms of lateral similarity variable, stream function, temperature, turbulent kinetic energy and its dissipation rate. Also, a, b, c, d, e, m, n, p and q are arbitrary constants. By substituting the above definitions (9) to (13) into Eqs. (2) to (5), we have:

$$a^2 b^2 x^{2m-2l-1}\left[(m-l)F'^2 - mFF''\right] = \frac{(\rho_l - \rho_v)}{\rho_l}.g + c_\mu \frac{a^3 b d^2}{e} x^{2p+m-q-3l}\left[\left(\frac{2KK'}{E} - \frac{K^2E'}{E^2}\right)F'' + \frac{K^2}{E}F'''\right] \tag{14}$$

$$abcx^{m+n-1-l}(n\theta F' - mF\theta') = \frac{c_\mu}{\sigma_t}\frac{a^2cd^2}{e} x^{2p+n-q-2l}\left[\left(\frac{2KK'}{E} - \frac{K^2E'}{E^2}\right)\theta' + \frac{K^2}{E}\theta''\right] \tag{15}$$

$$abdx^{m+p-l-1}(pKF' - mFK') = \frac{c_\mu}{\sigma_k}\frac{a^2d^3}{e} x^{3p-q-2l}\left[\left(\frac{2KK'}{E} - \frac{K^2E'}{E^2}\right)K' + \frac{K^2}{E}K''\right] + c_\mu \frac{a^4b^2d^2}{e} x^{2p+2m-q-4l}\frac{K^2F'^2}{E} - ex^qE \tag{16}$$

$$abex^{m+q-l-1}(qEF' - mFE') = \frac{c_\mu}{\sigma_\varepsilon} a^2d^2x^{2p-2l}\left[\left(\frac{2KK'}{E} - \frac{K^2E'}{E^2}\right)E' + \frac{K^2}{E}E''\right] + c_1c_\mu a^4b^2dx^{p+2m-4l}KF'^2 - c_2\frac{e^2}{d}x^{2q-p}\frac{E^2}{K} \tag{17}$$

The condensate layer thickness is a function of the ratio of conduction heat transfer to latent heat during phase change; consequently, energy balancing can be written as:

$$\int_0^x \lambda \left[\frac{\partial T}{\partial y}\right]_{y=0} dx = \int h_{fg}\, d\dot{m} \tag{18}$$

Using similarity variables in this equation yields:

$$-\lambda(T_{sat} - T_w)ac\theta'(\eta_\delta)\frac{x^{n-l+1}}{n-l+1} = \rho b h_{fg} x^m F(\eta_\delta) \tag{19}$$

To obtain the equations in similarity form, the role of variable x in Eqs. (14-17) and (19) should be eliminated. Therefore, the following equations must be satisfied:

$$\begin{cases} 2m - 2l - 1 = 0 \\ 2p + m - q - 3l = 0 \end{cases} \tag{20}$$

$$m + n - l - 1 = 2p + n - q - 2l \tag{21}$$

$$m + p\text{-}l\text{-}1 = 3p\text{-}q\text{-}2l = 2p + 2m\text{-}q\text{-}4l = q \tag{22}$$

$$m + q - l - 1 = 2p - 2l = p + 2m - 4l = 2q - p \tag{23}$$

$$n - l + 1 = m \tag{24}$$

By solving the above equations, the constant coefficients become:

$$l = 1, \quad m = \frac{3}{2}, \quad p = 1, \quad q = \frac{1}{2}, \quad n = \frac{3}{2} \tag{25}$$

Furthermore, the following relation should be satisfied so that the coefficients in Eqs. (14) to (17) can be omitted:

$$\frac{\frac{(\rho_l - \rho_v)}{\rho_l}.g}{a^2b^2} = \frac{ad^2}{eb} = \frac{a^3bd}{e} = \frac{ab}{\alpha c} = 1 \tag{26}$$

which results in:

$$a = 1, \quad b = \left[\frac{(\rho_l - \rho_v)}{\rho_l}.g\right]^{\frac{1}{2}}, \quad c = \left[\frac{(\rho_l - \rho_v)}{\alpha_l^2 \rho_l}.g\right]^{\frac{1}{2}}, \quad d = \frac{(\rho_l - \rho_v)}{\rho_l}.g, \quad e = \left[\frac{(\rho_l - \rho_v)}{\rho_l}.g\right]^{\frac{3}{2}} \tag{27}$$

Using these results through Eqs. (14-17) and (19), the set of similarity ordinary differential equations should take its final form:

$$F''' + \left(\frac{2K'}{K} - \frac{E'}{E}\right)F'' + \frac{E}{2c_\mu K^2}\frac{1}{Pr}\left(3FF'' - F'^2\right) + \frac{1}{Pr}\frac{E}{c_\mu K^2} = 0 \tag{28}$$

$$\theta'' + \frac{3}{2}\frac{\sigma_t E}{c_\mu K^2}(F\theta' - \theta F') + \left(\frac{2K'}{K} - \frac{E'}{E}\right)\theta' = 0 \tag{29}$$

$$K'' + \frac{\sigma_k E}{c_\mu K^2}\left(\frac{3}{2}FK' - KF'\right) + \left(\frac{2K'}{K} - \frac{E'}{E}\right)K' + \sigma_k F''^2 - \frac{\sigma_k E^2}{c_\mu K^2} = 0 \tag{30}$$

$$E'' + \frac{1}{2}\frac{\sigma_\varepsilon E}{c_\mu K^2}(3FE' - EF') + \left(\frac{2K'}{K} - \frac{E'}{E}\right)E' + c_1\sigma_\varepsilon \frac{E}{K}F''^2 - c_2\frac{\sigma_\varepsilon E^3}{c_\mu K^3} = 0 \tag{31}$$

Boundary conditions can be re-written in similarity form as below:

$$\eta = 0: \begin{cases} F = 0 \\ F' = 0 \\ \theta = 1 \\ K = 0 \\ E = 0 \end{cases}, \quad \eta = \eta_\delta: \begin{cases} F'' = 0 \\ \theta = 0 \\ K' = 0 \\ E' = 0 \end{cases} \tag{32}$$

where η_δ is the value of η at the condensate interface.

We also define a new variable which represents dimensionless eddy viscosity in similarity form. It is:

$$\nu_t^* = \frac{K^2}{E} \tag{33}$$

Moreover, Eq. (19) is changed into its similarity form as follows.

$$Ja_{turb} = -\frac{3}{2}\frac{F(\eta_\delta)}{\theta'(\eta_\delta)} \tag{34}$$

Here, Jacob number (Ja_{turb}) represents the ratio of sensible to latent heat transfer during liquid-vapor phase-change, which is:

$$Ja_{turb} = \frac{Cp\,\Delta T}{h_{fg}} \tag{35}$$

2.2 Solution Method

Evidently, the numerical solution of converted ODEs is much easier than PDEs with less computational efforts. However, the set of ordinary differential Eqs. (28-31) with their boundary conditions are non-linear and highly coupled. Furthermore, boundary conditions of equations reveal them to be singular at the plate surface. This property is the cause of vanishing turbulent kinetic energy and its dissipation rate at near wall region. Therefore, the Eqs. (28) to (31) are amenable to solve, and in this case, using common numerical schemes will not be helpful. Paullay *et al.* (1985) analyzed turbulent plane and radial jets using k-ε model in similarity form. They also had singularity problem in their equations, but according to governing momentum, turbulent kinetic energy and dissipation rate equations and related boundary conditions, they transferred singular point into infinite solution domain using a secondary transformation variable, and then solved them easily. However in the present problem, because of physical phenomena, mathematical model and equation properties mentioned above, we cannot use such methods. This means that a more efficient numerical scheme is required.

The governing equations in the present study (28-31) are a set of non-linear, non-homogenous, and third-order ordinary differential equation. Also, momentum, turbulent kinetic energy and its dissipation rate are coupled and must be solved coincidently. Moreover, we can see that there are some terms in the governing Eqs. (28-31) where K and E are in the denominator of the fraction, and we know that they are zero at many parts of computational domain. Hence, singularity is the main problem for this case. Dealing with non-homogenous governing equations and the presence of singular points within the computational domain also make the numerical scheme of ODEs very complicated.

There are several methods for solving the set of ODEs, but all of them diverge rapidly. There are also some asymptotical solutions for the problems including singular points (Paullay *et al.* 1985, Wen-xin and Li 1993), but these methods are only for single-phase cases. In this paper, we use Differential Transform Method (DTM). It is a suitable scheme for solving singular problems (Vedat, 2007). In this method, differential equation with n-order of derivations is converted to n+1 algebraic equations. Then, the set of algebraic equations are solved simultaneously. A code is developed using Maple software (version 18, 2014).

3. Results And Discussion

The results of computed average Nusselt number for different numbers of computational nodes are summarized in Table 1. The obtained results are for a turbulent film condensation on a vertical plate at Jacob number of 0.6. It is evident that a grid with 200 nodes is suitable for numerical computations.

Table 1 Mesh independency of computations for turbulent film condensation at Ja=0.6

Number of computational nodes	Average Nusselt number
50	0.51
100	0.48
150	0.41
200	0.402
250	0.401

At first, we used this method to solve the problem of turbulent planar jet for validation. Paullay *et al.* (1985) studied the same problem by considering a k-ε turbulence model. They reported that singular points appeared on the edge of the jet because the values of k and ε are set to be zero there. They transformed the singular points to infinity by transformation of coordinates and solved the equations asymptotically using central difference discretization. However, we solve the resultant ODEs directly by applying DTM method with less computational efforts.

Figs. 2 and 3 show the comparison of dimensionless velocity and turbulent kinetic energy profiles.

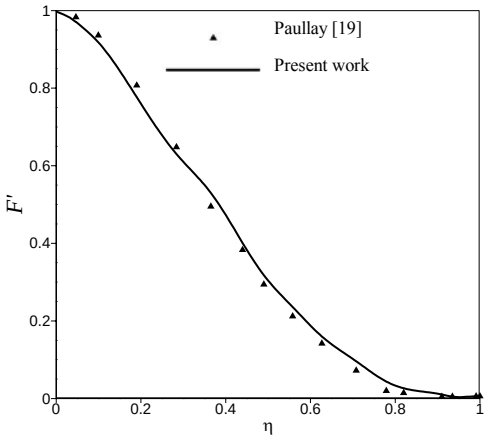

Fig. 2. Turbulent plane jet velocity profile, a comparison with Paullay work [19].

Based on the obtained results, we can say that the

results of the present DTM method are in good agreement with analytical asymptotic solution (Paullay *et al.* 1985).

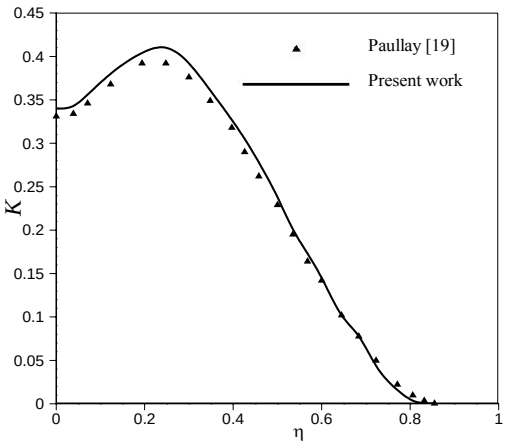

Fig. 3. Plane jet turbulent kinetic energy, a comparison with Paullay work [19].

The similarity solution of stream function of turbulent condensate layer is shown in Fig. 4. The stream function grows with increasing condensate thickness.

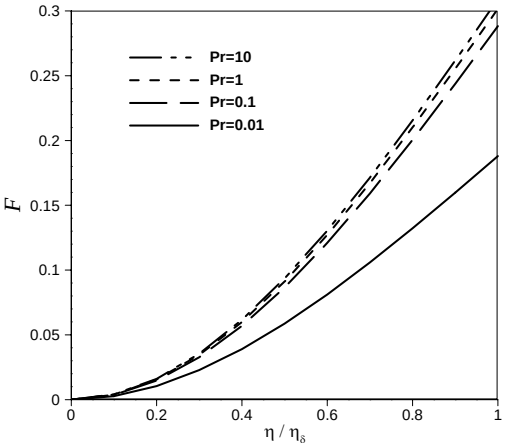

Fig. 4. Dimensionless stream function of turbulent condensate layer at different Pr numbers.

As it can be seen, the stream function increases with increase in Prandtl number. It is because in fluids with high Prandtl number, the momentum diffusivity is more than the thermal diffusivity and the resistance against fluid flowing is weak, therefore flowing power and consequently flow velocity increases at high Prandtl numbers (Fig. 5). Figs. 4 and 5 also show that when Prandtl number increases, the effect of momentum diffusivity decreases. This property is justifiable in mathematical and physical haunt. According to Eq. 30, when the Prandtl number grows, the two last terms vanish and therefore, the effect of Prandtl number becomes insensible. Also in turbulent flows, in fluids with high momentum diffusivity (high Prandtl number), the effect of fluid viscosity becomes negligible compared with eddy viscosity; therefore the effect of increasing Prandtl number is not significant.

According to variables definitions (10), velocity derivation represents the friction field. Friction field is shown in Fig. 6. As can be seen, change in friction field is not significant with Prandtl number variation. Therefore, it is preferred to draw two Prandtl number. The results show that in high Prandtl numbers, the friction value becomes smaller in the hole of condensate layer, especially near the wall. It can be explained that in high Prandtl numbers, the momentum diffusivity increases, therefore the resistance against liquid flow decreases and the flow friction takes smaller values.

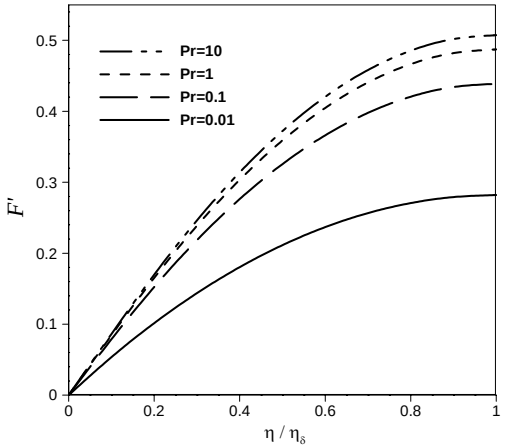

Fig. 5. Dimensionless velocity profile of turbulent condensate layer at different Pr numbers.

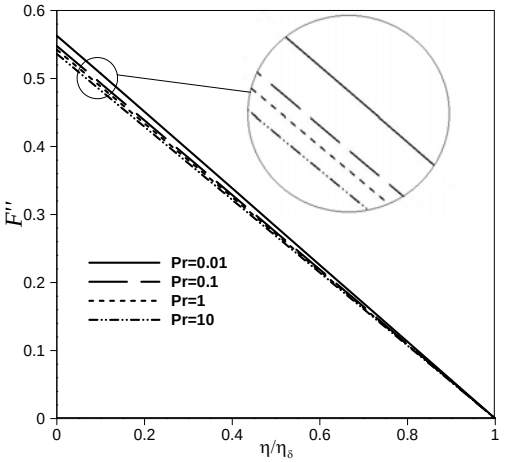

Fig. 6. Dimensionless friction field of turbulent condensate layer at different Pr numbers.

The lateral distribution of turbulent kinetic energy is shown in Fig. 7. The results show that turbulent kinetic energy increases linearly for the first 20% of lateral distance, then grows smoothly to 70% of condensate layer and finally, turbulent kinetic energy attains a constant value up to vapor-liquid interface at all Prandtl numbers. Therefore, the distribution of turbulent kinetic energy is not dependent on the type of fluid, but the order of magnitude of turbulent kinetic energy decreases with increase in Prandtl number. In fluids with high

Prandtl numbers, the value of velocity increases and its profile becomes more uniform and therefore, the turbulent generation decreases with high Prandtl numbers. Also in uniform velocity profile, the power of turbulent dissipation rate will grow (Fig. 8). According to Figs. 7 and 8 and Eq. 33, the turbulent eddy viscosity will increase along the lateral condensate layer and will decrease in high Prandtl numbers. According to the profiles of K and E and the definition of dimensionless eddy viscosity (Eq. 33), the results for eddy viscosity are shown in Fig. 9. As shown in this figure, eddy viscosity grows linearly at the first twenty percent of condensate layer and then its change becomes negligible.

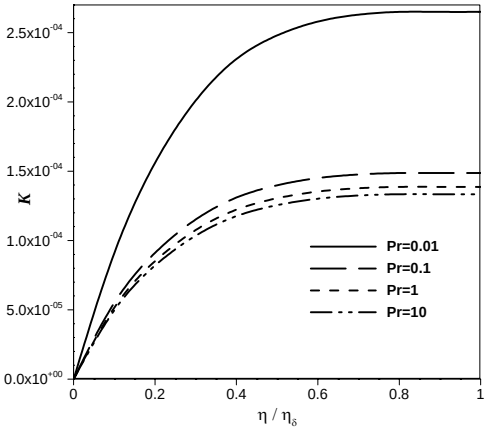

Fig. 7. Dimensionless turbulent kinetic energy across the condensate layer at different Pr numbers.

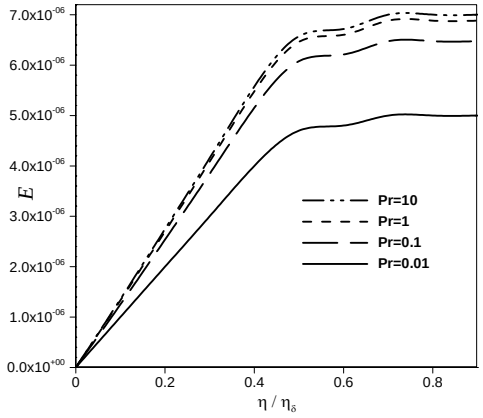

Fig. 8. Dimensionless dissipation rate of turbulent kinetic energy across the condensate layer at different Pr numbers.

In turbulent flows, the size and power of eddies are enhanced by distance from the solid walls, and consequently, the eddy viscosity increases rapidly from the wall. This is more considerable for low Pr number fluids in which the deterrence of viscosity is less compared with their thermal diffusivity. We can see in Fig. 9 that at all Pr numbers, the eddy viscosity increases sharply and then reaches a stable value after some oscillations close to the liquid-vapor interface.

It is also interesting to show the turbulent kinetic energy versus its dissipation rate along the lateral distance. In Fig. 10, we can see that from wall in most of the condensate layer, the growth rate of the turbulent kinetic energy is smaller than its dissipation rate, and near the vapor- liquid interface, the dissipation rate gets a constant value, while turbulent kinetic energy increases consistently. Paying attention to physical model, we can say that the effect of dissipation rate is significant because of the boundary condition on the solid wall and near the vapor- liquid interface.

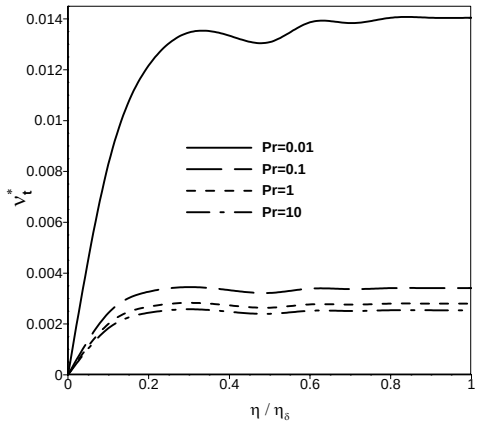

Fig. 9. Dimensionless eddy viscosity across the condensate layer at different Pr numbers.

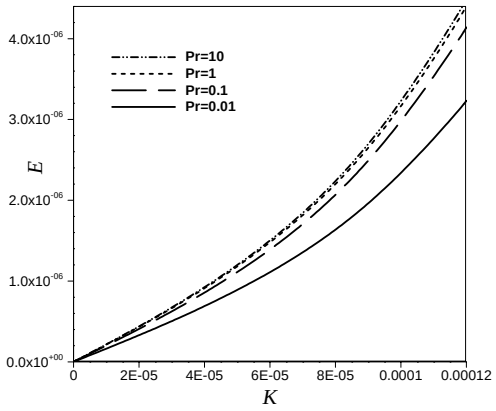

Fig. 10. Turbulent kinetic energy versus its dissipation rate for the condensate layer at different Pr numbers.

According to the vapor viscosity which is much smaller than liquid viscosity, there is no effective force against turbulent generation, therefore the turbulent kinetic energy increases continuously.

Average turbulent film condensation Nusselt number over a flat plate is shown in Fig. 11. The figure show how the Nusselt number changes versus Jacob number. When Jacob number increases, the ratio of heat transfer due to sensible temperature change is increased. On the other hand, increase in temperature gradient (Eq. 35), is due to increase in film thickness. Also in condensate layer with bigger thickness, the effect of conduction heat transfer decreases. Therefore, the ratio of convection heat transfer to conduction heat transfer

(which represents the Nusselt number) will grow by increasing the Jacob number. The figure also indicates that Nusselt number increases in high Prandtl numbers. This behavior is because in high Prandtl numbers, the effect of momentum diffusivity is more significant, therefore the heat transfer due to convection increases. At small Prandtl numbers, the change in Nusselt number with Jacob number is more considerable whereas by increasing the Prandtl number, this variation is reduced. The reason is that at low Prandtl numbers, the thermal diffusivity is more than momentum diffusion coefficient and thus, conductive heat transfer is dominant. As a result, the temperature gradient in the condensate film is larger and according to the definition of Jacob number, the variation of Nusselt number is more at low Prandtl numbers. It is also worth mentioning that for all Jacob numbers, the average Nusselt number of turbulent film condensation is larger than that of laminar flow at each Prandtl number.

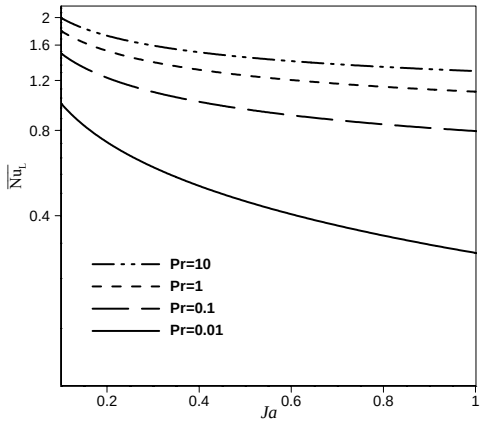

Fig. 11. Average Nusselt number versus Jacob number across turbulent condensate layer at different Pr numbers.

CONCLUSION

In this study, turbulent film condensation of pure stagnant vapor on a vertical flat plate was solved by using a similarity method. By defining four similarity variables, governing partial differential equation changed to set of ordinary differential equation, which is more amenable to solve. DTM method was used to remove singularity problem. Results of DTM method are in good agreement with creditable literatures. Results revealed that turbulent parameters are negligible near the wall (turbulent kinetic energy and its dissipation rate). In high Prandtl numbers, the velocity profile becomes smoother and the power of eddy production decreases. The turbulent kinetic energy increases almost linearly up to 0.2 of condensate film thickness and then tends toward a constant value near the liquid-vapor interface. The dissipation rate of kinetic energy also grows from the wall to 40% of condensate film thickness at all Prandtl numbers and then reaches a value after some oscillations. In all cases, the changes in small Prandtl numbers are more significant. We also found that among various flow parameters, the wall shear stress is less affected by the Prandtl number, since the velocity profile does not change significantly with the Prandtl number. We also obtained from the results that average Nusselt number on the surface in turbulent film condensation reduces by increasing Jacob number, since thermal equilibrium is achieved between the surface and the condensate film in high Jacob numbers.

REFERENCES

Avramenko, A., P. Sosnowski and A. Petronio (2014). Heat transfer at film condensation of stationary vapor with nanoparticles near a vertical plate. *Applied Thermal Engineering* 73, 391-398.

Avramenko, A., P. Sosnowski and A. Petronio (2015). Heat transfer at film condensation of moving vapor with nanoparticles over a flat surface. *International Journal of Heat and Mass Transfer* 82, 316-324.

Cha'o-Kuang C. and L. Yan Ting (2009). Turbulent film condensation in the presence of non-condensable gases over a horizontal tube. *International Journal of Thermal Sciences* 28, 1777–1785.

Chen, M. M. (1961). An analytical study of laminar film condensation. Part 1: flat plates, *J. Heat Transfer* 83, 48-54.

Cintolesi C., Petronio A. and V. Armenio (2017, December). Large-eddy simulation of thin film evaporation and condensation from a hot plate in enclosure: Second order statistics, *Int. J. Heat and Mass Transfer* 115, 410-423.

Gou, J., Wang B. and J. Shan (2017, August). Development of an analytical model for pure vapor down flow condensation in a vertical tube, *Nuclear Engineering and Design* 320, 346-360.

Huminic, G. and A. Huminic (2013). Numerical study on heat transfer characteristics of thermosyphon heat pipes using nanofluids. *Energy Conversion and Management* 76, 393-399.

Incropera, F. P. and D. P. DeWitt (2007). *Introduction to Heat Transfer*, 5th Edition, John Wiley & sons.

Kato, H., N. Shiwaki and M. Hirota (1968). On the turbulent heat transfer by free convection from a vertical plate. *Int. J. Heat Mass Transfer* 11, 117–1125.

Kays, W. M., M.E. Crawford and B. Weigand (2012). *Convective heat and mass transfer*, McGraw-Hill Education.

Kharangate, C. R. and I. Mudawar (2017). Review of computational studies on boiling and condensation, *Int. J. Heat and Mass Transfer* 108(Part A), 1164-1196.

Koh, J. C. Y., E. M. Sparrow and J. P. Hartnett (1961). The two phase boundary layer in laminar film condensation, *Int. J. Heat Mass Transfer* 2, 69-82.

Lee, J. (1964). Turbulent film condensation, *AIChe Journal* 10(4) 540–544.

Liu, Z., Y. Li and R. Bao (2010). Thermal performance of inclined grooved heat pipes using nanofluids. *International Journal of Thermal Sciences* 49, 1680-1687.

Mendez, F., J. J. Lizardi and C. Trevino (2000). Laminar film condensation along a vertical fin. *J Heat & Mass Transfer* 43, 2859-2868.

Michael, A., G. Rose and L. C. Daniels (1989). Forced convection condensation on a horizontal tube-experiments with vertical down flow of steam. *ASME Journal of Heat Transfer* 111, 792-797.

Nakayama, A. and H. Koyama (1984). Turbulent film condensation on a horizontal circular cylinder. *Int. Comm. Heat Mass transfer* 11, 115-126.

Paullay, A. J., R. E. Melnik, A. Rubel and S. Rudman (1985). Similarity solutions for plane and radial jets using a k-ε turbulence model. *ASME Journal of Fluids Engineering* 107, 79-85.

Sarma, P. K., B. Vijayalakshmi, F. Mayinger and S. Kakac (1998). Turbulent film condensation on a horizontal tube with external flow of pure vapors. *Int. J. Heat Mass Transfer* 4, 537–545.

Shekriladze, I. G. and V. I. Gomelauri (1966). Theoretical study of laminar film condensation of flowing vapor. *Int. J. Heat Mass Transfer* 9, 581–591.

Shen, Q., D. Sun, S. Su, N. Zhang and T. Jin (2017, May). Development of heat and mass transfer model for condensation, *Int. Communications in Heat and Mass Transfer* 84, 35-40.

Sheng, A. Y. and L. Yan Ting (2005). Turbulent film condensation on a non-isothermal horizontal tube effect of eddy diffusivity. *Applied Mathematical Modelling* 29, 1149–1163.

Sosnowski, P., A. Petronio and V. Armenio. (2013). Numerical model for thin liquid film with evaporation and condensation on solid surfaces in systems with conjugated heat transfer. *International Journal of Heat and Mass Transfer* 66, 382-395.

Sparrow, E. M. and J. L. Gregg (1959). A boundary-Layer treatment of laminar film condensation. *J Heat Transfer* 81, 13-18.

Swartz, M. M and S. C. Yao (2017). Experimental study of turbulent natural-convective condensation on a vertical wall with smooth and wavy film interface, *Int. J. Heat and Mass Transfer* 113, 943-960.

Vedat, S. E. (2007). Differential Transformation Method For Solving Differential Equations of Lane-Emden Type. *Mathematical and Computational Applications* 12, 135-139.

Wen-xin, H. and W. Li (1993). Similarity solutions of round jets and plumes. *Applied Mathematics and Mechanics* 14, 649-658.

Wilcox, D. C. (1994). *Turbulence Modeling for CFD*. DCW Industries Inc.